

The Implementation in VISSIM REALTIME of an Active Electromagnetic Damper Controller for Lightweight Electric Vehicles

Alista Fow and Mike Duke
Department of Engineering,
University of Waikato,
Hamilton, New Zealand,
ajf8@students.waikato.ac.nz.

Mike Duke
Department of Engineering,
University of Waikato,
Hamilton, New Zealand
Dukemd@waikato.ac.nz

Abstract— The use of linear electromagnetic active damper units in the suspension system of a lightweight electric vehicle offers many advantages over conventional passive, semi-active and active hydraulic dampers. While full active hydraulic systems have been commercially available in automobiles for many years, the linear electromagnetic active damper offers a lower weight system with a much reduced power demand. However an active system requires the use of a controller to adjust the power output to the damper unit. This unit must process signal inputs and provide an output solution within a short time period, often 5 milliseconds or less. By using VISSIM REALTIME, a controller was built that controlled a scale linear electromagnetic damper using Karnopp's Skyhook algorithm. This had to deal with issues such as accelerometer drift and signal to noise ratio. These required simple but fast techniques to provide useful information to the damper in a useful timeframe. This controller-damper combination proved effective in reducing the vibration experienced by the sprung mass and was more effective than an ideal passive damper at all frequencies tested by at least a factor of three.

Keywords-component; Active, Suspension, Modelling, Simulation.

I. INTRODUCTION

In modern automobiles the standard, passive suspension system uses hydraulic dampers and coil springs. The objective of the suspension system is to minimise passenger vibration, maximise the tyre contact forces with the road surface and achieve this with limited suspension travel [1]. Modern passive suspension systems are therefore a compromise of the three requirements.

An alternative to passive suspension systems are fully active or semi-active suspension systems that control the forces applied to the vehicle and thereby offer significantly improved performance. However, a fully active hydraulic system can require significant power to operate. Kim, 2002, calculated that the power required to operate such a system on a typical passenger vehicle is 3.8 kW [2]. This research focusses on active suspension systems for electric vehicles. For electric vehicles as proposed by [3], [4], [5] and [6], the range of the electric vehicle depends upon the energy consumption. From Duke [6], the power consumption of desired electrical vehicles can range from approximately 5 – 11 kW, so a conventional active system would greatly reduce the range of such vehicles.

In recent years semi-active dampers have become available that offer improved performance compared to conventional passive dampers but at far low power consumption than fully active hydraulic systems. Skyhook damping, as proposed by Karnopp and Crosby in [7], has been shown to offer greatly improved vibration performance compared to passive parallel systems (Fig. 1). Consequently, they have been used in a number of production automobiles in recent years. These semi-active dampers can be switched on and off or continuously varied under the command of a control algorithm. Most commercial magnetorheological semi-active dampers give effective Skyhook damping with little power usage. The main problem with the magnetorheological dampers is that they only dissipate the vehicle body energy whereas an ideal suspension system would also add energy to control vehicle body roll, dive and squat.

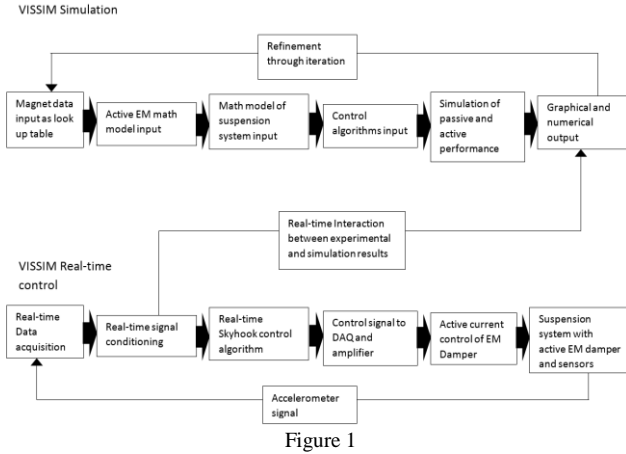


Figure 1

Electromagnetic (EM) active dampers could potentially offer the same advantages as a magnetorheological semi-active damper but with the possibility of adding energy to better control vehicle body motion. To reduce energy demand in an active EM suspension system a passive coil spring in parallel to the active damper is required that provides static support force and a dynamic force proportional to the relative displacement between the vehicle body and wheel as shown in Fig.2. This work therefore focusses on whether an active EM damper with passive spring can offer similar or improved performance compared to a conventional passive suspension. The approach taken in the research was to first develop mathematical models of the passive and active systems, simulate and their performance and compare with experimental results. The key question being what is the best way of achieving the simulation and experimental results.

II. METHODOLOGY

There is a wide range of options for simulation and experimentation of control systems. In academia, probably the most common approach is to use MATLAB software for simulation in conjunction with National Instruments (NI) hardware for experimentation. However, the cost of the complete system can be prohibitive for researchers with minimal research funding. Alternative microcontrollers such as Arduino are now available that could potentially deliver the control algorithm and experimentation at low cost. However, time is required to configure the hardware and write the control algorithm coding and there is no simulation capability. After reviewing various options, VISSIM was chosen as it could be used for simulation and experimentation simultaneously, was, flexible, fast, low cost, easy to configure with hardware and featured real-time control.

VISSIM is a member of a class of programming languages that offers a graphical programming interface using block diagrams. Other languages with a similar style of interface include MATLAB SIMULINK and LABVIEW. The advantages of this style of programming include ease of use, familiarity due to the similarity to wiring diagrams and the elimination of bugs due to basic syntax errors. Another

potential benefit is the speed of prototyping control systems and models of real word simulations by non-specialist computer programmers. The process of using VISSIM for both simulation and experimentation, using Real-time control is shown in figure 3. The one integrated model has the simulation, real-time control of the physical system and sensor data.

III. THE HARDWARE IMPLEMENTATION

A single degree of freedom active damper was constructed and is shown in figure 2. The damper element was constructed using a coil of 120 turns in three layers of 40 windings each wound on to a PVC core. The sprung mass was 1kg and had a natural frequency of 1.6 Hz. A Neodymium magnet with N35 rating and of physical dimensions 28mm length and 19mm diameter was attached to the sprung mass and this magnet produced a nominal magnetic field at the surface of the poles of 0.5733T. The whole assembly was mounted upon a vibration platform.

The magnet was axially magnetised and assumed to have radial symmetry. The model of the magnet was used to generate a lookup table of the force generated by the damper as described in [8] using the well-known thin walled solenoid model of a permanent magnet to determine the magnetic field at any point, as described by [9]. Experimentation determined that there was a better than 95% agreement between the predicted forces and the measured forces.

The sprung mass had an Analogue Devices ADXL325 accelerometer mounted upon the sprung mass. This was capable of measuring accelerations of $\pm 5g$ in all three axis. The signal input was entered into the computer through a Measuring Computing PCI-DAS6014 data acquisition board which was installed in an IBM based computer. This board was chosen for the ability to output analogue signals that would then drive the active damper: due to the ability to use software that would allow rapid control prototyping and due to

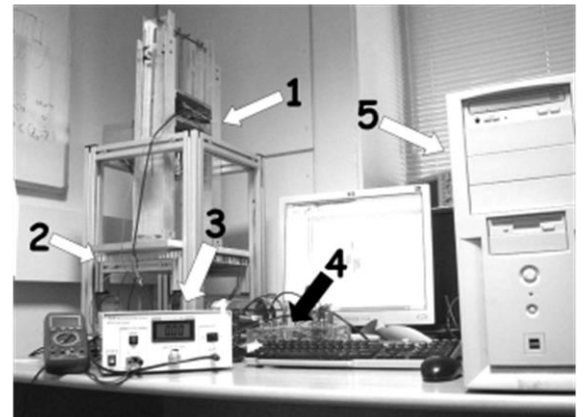


Figure 2 The experimental apparatus for an active damper. (1) - the spring, damper, sprung mass and accelerometer, (2) The vibration surface. (3) The current amplifier. (4) The data input/output ports. (5) The computer with VISSIM REALTIME.

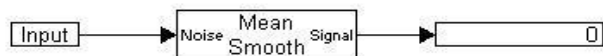
financial benefits of using equally capable, but much lower priced equipment. To verify the results of the damper a pre-calibrated PCB356A02 accelerometer is used in conjunction with a COCO80 signal analyser.

IV. THE SOFTWARE IMPLEMENTATION

As previously stated, VISSIM REALTIME was chosen for both simulation and experimentation of the damper model. Figure shows one of the main advantages of VISSIM's block diagram approach compared to standard coding. The block diagram took approximately 1/10 of the time required to write the coding and had much less chance or errors and debugging.

REALTIME has the capability of inputting data in while a process is occurring, of manipulating that data and then providing a control signal in a timely manner. The computer that was used was easily capable to process the controller signals at 2,000 Hz, or over 10,000 Hz when a user display was not required.

Due to the graphical nature of the language and the use of prewritten and tested blocks of code the programming demands and complexity are greatly reduced when compared



(a)

```

%define values in main program
max_data_size = 1000;
data_value = zeros(max_data_size);
count_number=1;
number_entries=0;

% enter data and call the function in main program
mean_value = running_mean(measured_value);

% Determine the running mean in a separate M file
function [data_mean]=running_mean(input_value)
data_value(count_number) = input_value;
count_number = count_number + 1;
if count_number > max_data_size
    count_number = 1;
end
number_entries = number_entries + 1;
if number_entries >max_data_size
    number_entries = max_data_size;
end
data_value = sum(datavalue);
data_mean = data_value/number_entries.;
end
  
```

(b)

Figure 3 – A program in (a) VISSIM and (b) MATLAB to determine the running mean of the previous 1,000 data entries.

to using a procedural language such as MATLAB. Figures 1(a)_a and 1(b) both produce a running mean of a data stream for the last 1,000 measurements. They also both have the capacity to produce the running mean from start up, while the number of data points less than 1,000.

Two accelerometers were used on the sprung mass. The ADXL325 was used to provide a signal to REALTIME as this is a type of accelerometer that may be used in a practical situation. And the PCB356A02 accelerometer was a laboratory quality precalibrated device that was used to validate the results. To calibrate the ADXL325 a test run was conducted on the sprung mass with both accelerometers attached the r.m.s. values of both accelerometers were taken and a magnification factor was determined. As there was no code block in VISSIM REALTIME, one was constructed using three code blocks in series to square the values, to perform a mean smoothing function and determine the positive square root.

As previously stated the algorithm chosen to implement for a one degree of freedom active electromagnetic damper was the Skyhook damper .The force generated by the active element is determined by (1)

$$F = -b\dot{x} \quad (1)$$

where F is the force generated in Newtons, b is the damping coefficient of the damper N s/m and \dot{x} is the velocity of the sprung mass relative to a fixed inertial point in m/s.

The control algorithm required the input of the absolute velocity of the sprung mass. This was achieved by integrating the acceleration.

The sprung mass had an Analogue Devices ADXL325 accelerometer mounted upon it. This was capable of measuring accelerations of $\pm 5g$ in all three axis. The signal input was entered into VISSIM REALTIME through a Measuring Computing PCI-DAS6014 data acquisition board which was installed upon an IBM based computer. This accelerometer has a built in signal conditioning amplifier and does not require any additional signal processing before entry into REALTIME.

To calibrate the accelerometer a run was conducted on the vibration apparatus with both the ADXL325 accelerometer and the pre-calibrated PCB356A02 accelerometer. The output from the ADXL325 accelerometer was recorded directly to VISSIM REALTIME while the output from the PCB356A02 was recorded with a COCO80 Signal Analyser. This data was then imported into VISSIM REALTIME. Both data sets were then displayed superimposed. As both accelerometers had been measuring the same input signal, the phase of the ADXL325 signal was then adjusted so that both signals were synchronised. The signal of the ADXL325 accelerometer was then amplified until both of the waveforms recorded a good

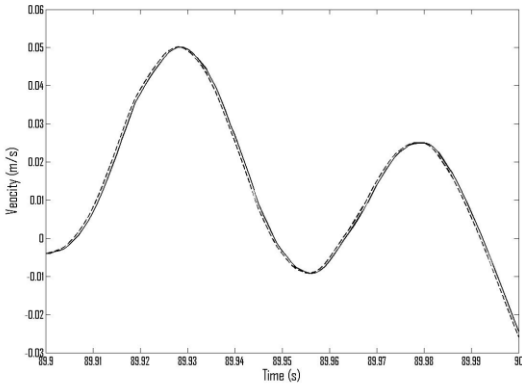


Figure 4: Comparison of velocities between the custom and VISSIM integrators. The VISSIM integrator with 4th order Runge-Kutta interpolation is represented by the solid line. The dashed line is the velocity from the custom integrator

agreement. It was determined that the ADXL325 signal had to be magnified 81 times to produce the same signal as the PCB356A02. The calibration was accordingly set as $1 \text{ V} = 81 \text{ m/s}^2$.

With the calibration of the accelerometer the velocity of the accelerometer could then be determined by integrating the acceleration output signal. A custom integrator was constructed so as to reduce the processor time required. No interpolation was included so as to also reduce the processor time. This was considered unnecessary as self-correction software was included in the acceleration signal. The total implementation took four code blocks. Using the same accelerometer test data as for the previous examples, a comparison was performed between the custom integrator and the VISSIM integrator using a 4th order Runge-Kutta algorithm to perform interpolation. In figure 4 a comparison was performed between the two signals. Due to the nature of integrated signals to drift after a period, the comparison shown is between 89.9 and 90 s. As is observed the two signals have a very close relationship, the major difference being a phase shift of 0.5 ms.

In the use of accelerometers there is always a measure of accelerometer ‘drift’ where the accelerometer measures a change of acceleration even when the equipment is motionless. In figure 5 it can be seen that there is an offset in the signal and that there is an average variation in the signal of

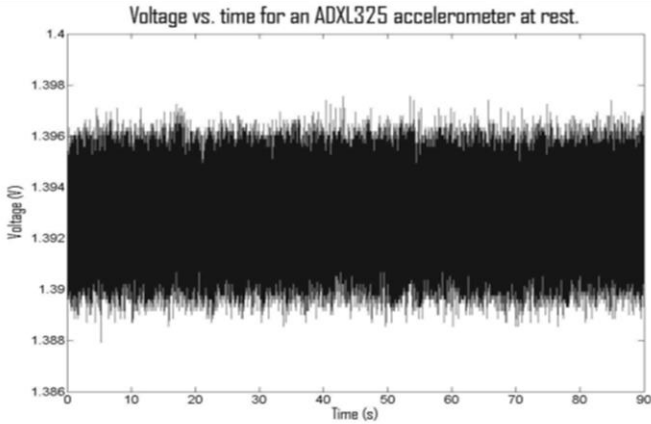


Figure 5 The unprocessed signal of the ADXL325 accelerometer.

TABLE 1: THE SIGNAL DELAY DUE TO THE USE OF SIGNAL FILTERS

Filter	Delay (ms)
Buttersworth , 5th order	110
Bessel, 2nd order	57
Chebyslev, 2nd order	33
Inverse Chebyslev, 4th order	44
Differentiator	393
Hilbert Transform	57

$\pm 0.003 \text{ V}$. This produces a variation of the measured acceleration of $\pm 0.24 \text{ m/s}^2$. By use of subtracting running mean for the total data run it is possible to remove the offset for previously measured data runs. However using such a long period is not possible during real time control. By use of subtracting the running mean over the previous seconds the offset could be removed for real time use by self-leveling the signal. This was achieved by using two code blocks.

Integration of the offset signal is shown in figure 6 as the grey line. In this typical drift measurement the motionless object is recorded as traveling with a peak velocity of 0.6 m/s and an mean absolute velocity of 0.2645 m/s. The signal is unuseable by the damper controller in this form as the drift figures can exceed the quantities being measured.

Several filters were included in the VISSIM package whose function is to smooth the signal. These included Besel, Buttersworth, Chebyslev, Differentiator, Hilbert Transform and Inverse Chebyslev filters. For a filter to be effective it was determined that the maximum signal delay allowable was 10ms. As can be seen from table 1 it can be seen that none of the filters available could meet these performance demands.

By repeating the self-leveling function previously used for the acceleration signal offset and applying the same function to the integrated velocity signal it was possible to reduce the noise in 1 ms, as shown by the dark line in figure 6. In the final instance an effective control damper was created using 10 code blocks. A more complete simulation of a two degree of freedom system with Skyhook controller and modelling of

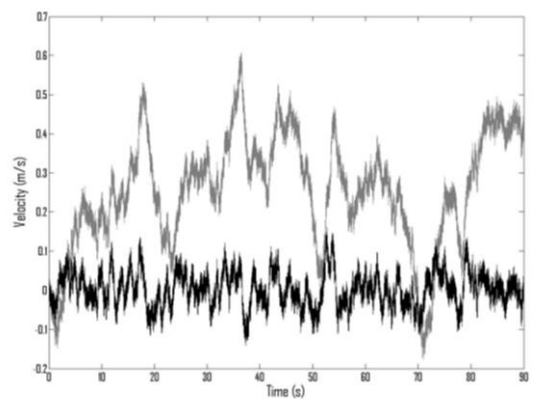


Figure 6: The random drift signal with no self-leveling and 1 s self-leveling. The light grey signal was without smoothing and the black signal was with self-leveling with a 1 second running mean.

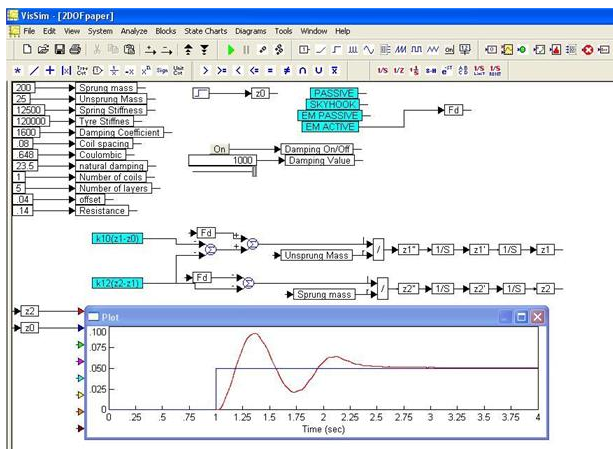


Figure 7 – A two degree of freedom simulator with active e.m. damping, using VISSIM.

the magnetic field for multiple magnets and multiple coils, each with multiple layers of windings, as well as Coulombic Damping and natural viscous damping requires a total of less than 60 code blocks.

The final block diagram for a two degree of freedom electric vehicle damper for determination of motions is given in figure 7. The results of experimentation between the modelled motions of a system and the experimentally determine results are given in figure 8. The use of VISSIM REALTIME was successful and provided useful, repeatable and verifiable results.

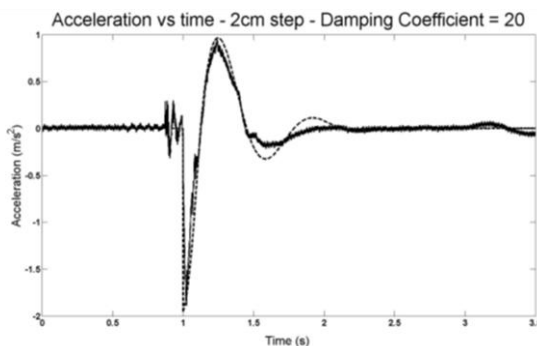


Figure 8.- Acceleration vs time for a 2 cm bump with an active damping coefficient of 20 N m/s. "—" measured. "---" modelled.

V. CONCLUSIONS

In order to investigate an active electromagnetic damper, simulation and experimentation. In the implementation of the active damper implementation in both hardware and software was required.

Use of VISSIM and VISSIM REALTIME allowed for the rapid development of both the controllers and simulators for a variety of active, semi and passive electromagnetic dampers and allowed for easy scaling to real world automotive damping. The use of VISSIM greatly reduced the programming time and further reduced the time spent on debugging. These advantages allowed more time to be spent of experimentation and simulation rather than traditional coding. A successful active damper controller was tested and verified using this software strategy.

REFERENCES

- [1] Williams, D. E. and W. M. Haddad., (1997), *Active suspension control to improve vehicle ride and handling*. Vehicle System Dynamics, 29, pp. 1-24.
- [2]]Kim, S. and Okade, (2002), Variable resistance type energy regenerative damper using pulse width modulated step-up chopper. Journal of Vibration and Acoustics, 124, pp. 110-5.
- [3] Qiu, H., Liang, S., Qi, Z., & Qin, H. (2012, November). A novel design of an in-situ steering for a 4-wheel independent steering in a 4-in-wheel-motor Drive Electric Vehicle. In *Mechatronics and Machine Vision in Practice (M2VIP), 2012 19th International Conference* (pp. 42-45). IEEE.
- [4] He, P., Dong, Z., Liang, S., Qi, Z., & Qiu, H. (2012, November). A novel design of all-wheel independent steering using regenerative in-wheel motors for a four in-wheel-motor drive electric vehicle. In *Mechatronics and Machine Vision in Practice (M2VIP), 2012 19th International Conference* (pp. 51-55). IEEE.
- [5] Duke, M., Andrews, D., & Anderson, T. (2009). The feasibility of long range battery electric cars in New Zealand. *Energy Policy*, 37(9), 3455-3462.
- [6] Duke, M., & Anderson, T. N. (2008). The potential for battery electric vehicles in New Zealand.
- [7] Karnopp, D., M. Crosby, and R. Harwood, (1974), *Vibration control using semi-active force generators*, Transactions of the ASME: Journal for Industry for Industry, 96(2), pp. 619-26 .
- [8] Fow, A. (2014), *Investigation into lowpower active electromagnetic damping for automotive applications*. Unpublished doctoral dissertation, University of Waikato, Hamilton, New Zealand.
- [9] Kuns, K. (2007), *Calculation of magnetic field inside plasma chamber*. UCLA report, 2(3), pp. 1-11.